

# Comparison of Different Spatial Regression Methods for Predicting Organic Matter Content in Soil

**Xumeng Zhang**

College of Resources and Environment, Shanxi Agricultural University, Taigu 030801, China

**Wuping Zhang** (✉ [zwping@126.com](mailto:zwping@126.com))

College of Software, Shanxi Agricultural University, Taigu 030801, China

**Mingjing Huang**

Dryland Agriculture Research Center, Shanxi Agricultural University, Taiyuan 030031, China;

**Li Gao**

College of Resources and Environment, Shanxi Agricultural University, Taigu 030801, China

**Lei Qiao**

College of Resources and Environment, Shanxi Agricultural University, Taigu 030801, China

**Guofang Wang**

College of Resources and Environment, Shanxi Agricultural University, Taigu 030801, China

**Linlin Yan**

College of Resources and Environment, Shanxi Agricultural University, Taigu 030801, China

---

## Research Article

**Keywords:** Spatial Regression Methods, Predicting Organic Matter Content, Soil, prediction accuracy, soil organic matter, technical support

**Posted Date:** January 6th, 2022

**DOI:** <https://doi.org/10.21203/rs.3.rs-1220228/v1>

**License:** © ⓘ This work is licensed under a Creative Commons Attribution 4.0 International License.

[Read Full License](#)

---

1 **Comparison of Different Spatial Regression Methods for Predicting**

2 **Organic Matter Content in Soil**

3 **Xumeng Zhang<sup>1</sup>, Wuping Zhang<sup>2, \*\*</sup>, Mingjing Huang<sup>3,4</sup>, Li Gao<sup>1</sup>, Lei Qiao<sup>1</sup>,**

4 **Guofang Wang<sup>1</sup>, Linlin Yan<sup>1</sup>**

5 1. College of Resources and Environment, Shanxi Agricultural University,

6 Taigu 030801, China.

7 2. College of Software, Shanxi Agricultural University, Taigu 030801, China.

8 3. Dryland Agriculture Research Center, Shanxi Agricultural University, Taiyuan

9 030031, China.

10 4. State Key Laboratory of Integrative Sustainable Dryland Agriculture (in

11 preparation) , Shanxi Agricultural University, Shanxi Institute of Organic

12 Dryland Farming, Taiyuan 030031, China

13

14

15

16

17

18

19

---

\* College of Software, Shanxi Agricultural University, Taigu 030801, China.

Correspondence and requests for materials should be addressed to W.P.

Zhang (email:zwping@126.com)

20 **Dynamic changes in soil organic matter content affects the sustainable**  
21 **supply of soil water and fertilizer and impacts the stability of soil**  
22 **ecological function. Understanding the spatial distribution**  
23 **characteristics of soil organic matter will help deepen our understanding**  
24 **of the differences in soil organic matter content, soil formation law; such**  
25 **understanding would be useful for rational land use planning. Taking**  
26 **terrain data, meteorological data, and remote sensing data as auxiliary**  
27 **variables and the ordinary Kriging (OK) method as a control, this study**  
28 **compares the spatial prediction accuracies and mapping effects of**  
29 **various models (MLR, RK, GWR, GWRK, MGWR, and MGWRK) on soil**  
30 **organic matter. Our results show that the spatial distribution trend of soil**  
31 **organic matter predicted by each model is similar, but the prediction of**  
32 **composite models can reflect more mapping details than that of unitary**  
33 **models. The OK method can provide better support for spatial prediction**  
34 **when the sampling points are dense; however, the local models are**  
35 **superior in dealing with spatial non-stationarity. Notably, the MGWR**  
36 **model is superior to the GWR model, but the MGWRK model is inferior to**  
37 **the GWRK model. As a new method, the prediction accuracy of MGWRK**  
38 **reached 47.72% for the OK and RK methods and 40.08% for the GWRK**  
39 **method. The GWRK method achieved a better prediction accuracy. The**  
40 **influence mechanism of soil organic matter is complex, but the MGWR**  
41 **model more clearly reveals the complex nonlinear relationship between**

42 **soil organic matter content and factors influencing it. This research can**  
43 **provide reference methods and mapping technical support to improve**  
44 **the spatial prediction accuracy of soil organic matter.**

45

46 Soil organic matter (SOM) is a crucial component of the soil carbon pool  
47 [1-3]. It features plant growth and is heavily utilized to evaluate soil quality [4].  
48 SOM is affected by managerial, topographic, and climatic factors, as well as  
49 others [5, 6]. Studies on the spatial distribution of SOM are helpful for  
50 understanding regional soil quality, and have significance in the improvement  
51 of spatial organic matter content and land resource management [7, 8]. The  
52 spatial distribution of SOM usually has spatial variation due to the influence of  
53 structural and random factors; that is, the existence of spatial non-stationary  
54 characteristics leads to uncertainty in the modeling process [9]. Therefore, it is  
55 difficult to accurately simulate the spatial distribution of SOM.

56 There are numerous methods for predicting SOM; however, the commonly  
57 used method is the ordinary Kriging (OK) method, which can simulate the  
58 distribution of soil organic matter in the entire region through limited point data.  
59 It fully considers spatial variability and theoretically interpolates errors.  
60 However, the OK method is dependent on the quality of the sampling point and  
61 is restricted without considering the influence of other factors [10]. The  
62 relationship between soil properties and environmental variables is an  
63 extremely complicated non-linear relationship [11], and the accurate

64 expression of this relationship vital to improving the prediction accuracy.

65 Therefore, auxiliary variables are introduced into the prediction model.  
66 Chen et al. [12] introduced surface albedo to participate in the spatial  
67 prediction modeling of SOM. Li et al. [13] used 11 environmental factors from  
68 climate, terrain, and vegetation combined with principal component analyses  
69 as predictors of SOM. In addition to considering quantitative auxiliary variables,  
70 Li et al. [14] integrated qualitative auxiliary variables, such as soil texture. The  
71 results proved that the introduction of auxiliary variables can significantly  
72 improve the prediction accuracy of SOM. Additionally, many studies have  
73 proved that the introduction of terrain, vegetation, and climate factors as  
74 auxiliary variables can significantly improve the prediction accuracy of soil  
75 properties [15-17].

76 Among various prediction methods with auxiliary factors, Lopez [18] used  
77 the multiple linear regression (MLR) method to combine the blue bands of  
78 remote sensing images and soil properties to predict the spatial distribution of  
79 SOM, pH, and K. Duan et al. used the CoKriging method combined with  
80 auxiliary variables to predict SOM [19]. The results showed that the correlation  
81 coefficient ( $r$ ) increased from 0.1 to 0.70 and 0.69. Hengl et al. showed that  
82 regression Kriging (RK) combined with the digital elevation model (DEM) was  
83 more accurate than ordinary Kriging (OK) in predicting SOM and tillage  
84 thickness [20]. However, the spatial non-stationary characteristics of soil  
85 attributes limit the accuracy of global models such as the ordinary least

86 squares (OLS) model. The geographically weighted regression (GWR) model,  
87 a local model widely used in the field of economic geography, has been  
88 introduced into the study of soil attribute heterogeneity, and has gradually  
89 become a vital tool for such research.

90 Niu et al. proved that the introduction of a GWR model greatly improved  
91 the interpretation of driving factors compared with the traditional OLS model  
92 [21]. In a study of prediction methods for farmland SOM in the Weibei dryland  
93 area, Yu et al. indicated that the correlation coefficient  $R^2$  increased to 0.902  
94 using the GWR model [22]. Ding et al. used the GWR model to explore the  
95 spatial distribution of soil organic carbon (SOC) and its influencing factors in  
96 the Yihe River basin [23]; these results showed that the GWR model simulated  
97 the spatial distribution of SOC and analyzed the different effects of different  
98 factors on different terrain units.

99 Geographically weighted regression kriging (GWRK) is a combination of  
100 the GWR and OK models, and is an improvement of the RK model. GWRK  
101 optimizes the residual error of the GWR model and reflects local details  
102 masked by global models such as RK. Yang et al. [24] studied the spatial  
103 distribution of SOM based on the GWRK model. Compared to the RK model,  
104 the GWRK model considered the location of the sample points, refined the  
105 mapping effect, and improved the overall accuracy. Liu et al. [25] compared  
106 several different spatial geographic technologies to predict SOC reserves and  
107 concluded that the GWRK model significantly reduces the error of the model

108 and is an effective method for mapping SOC storage in a local range. Ye  
109 conducted research that indicated that GWRK can be regarded as the best  
110 method for predicting SOC when the data samples are sufficient [26].

111 The multi-scale geographic weighted regression model (MGWR) was  
112 proposed by STWART et al. in 2017 [27]. Each variable in the model has a  
113 multi-scale optimal bandwidth. MGWRK is analogous to the GWRK model,  
114 which not only considers the multiple scales of the MGWR model, but also  
115 optimizes the regression residuals of the model. The model is worth exploring  
116 in terms of predicting soil properties and mapping.

117 In previous studies, it was necessary for scholars to explore the  
118 application of different models in soil spatial attributes, which provides  
119 mentalities for the development of spatial prediction and mapping technology,  
120 but it is still confined to the selection of environmental factors, the construction  
121 of models, and the spatial scale of different variables [28-30]. The complexity  
122 of the external environment determines that the applicability of each model is  
123 different. Under different environments, the prediction performance  
124 conclusions of different SOM models are not universal. For the spatial  
125 prediction of research objects, we should explore it and select the most  
126 appropriate method. In this study, ten factors in three categories—terrain data,  
127 meteorological data, and remote sensing data—were selected as  
128 environmental covariates for modeling, and different spatial prediction  
129 methods (OK, MLR, RK, GWR, GWRK, MGWR, and MGWRK) were

130 compared to provide technical support and a theoretical basis to accurately  
131 predict the spatial distribution of SOM and reasonable improvement of soil  
132 organic matter content in cultivated land.

133

## 134 **Materials and Methods**

135 **Study area.** Lingshi County is in the central part of Shanxi Province, the  
136 southernmost tip of Jinzhong City (110° 20' to 112° E, 36° 40' to 37° N).  
137 It is part of the Loess Plateau, with undulating mountains and ravines. The  
138 county covers an area of 1206 km<sup>2</sup>. The region consists of mountains on the  
139 East and West and the Fenhe Valley in the middle, which naturally forms a  
140 three-level ladder: the middle mountain area, hilly area, and Pingchuan Valley,  
141 of which the hilly area accounts for the largest proportion of the total area  
142 (57.6 %). The study area has a warm temperate continental climate, which is  
143 windy in the spring, hot and rainy in the summer, cool and refreshing in the  
144 autumn, and cold and a little snowy in the winter. The average annual  
145 temperature is 10.8 °C, the average annual precipitation is 473.5 mL, and the  
146 frost-free period is 156-day-long. The entire territory has 246 km<sup>2</sup> of cultivated  
147 land and is abundant in biological and mineral resources.

148 **Soil Data Collection and Auxiliary Variables Sources.** A total of 2245  
149 sample points were obtained before crops were planted in the autumn of 2009.  
150 According to the “Rules for soil quality survey and assessment”  
151 (NY/t1634-2008), the “s” method was used to arrange points in each field. The

152 sampling depth was 0–20 cm, and the sampling points are shown in Figure 1.  
 153 SOM was determined using the external heating potassium dichromate  
 154 method [31]. The digital elevation model (DEM) was obtained from the  
 155 Geospatial Data Cloud website (<https://www.gscloud.cn>) and each terrain  
 156 factor was extracted from the DEM. Annual mean precipitation (PRE) and  
 157 annual mean temperature (TEM) were extracted from meteorological datasets,  
 158 and the annual net primary productivity (NPP) and normalized differential  
 159 vegetation index (NDVI) were extracted from remote sensing datasets, both of  
 160 which were obtained from the Resource and Environment Science and Data  
 161 Center (<https://www.resdc.cn>). The environmental covariates are presented in  
 162 Table 1.

163 **Methods for estimating SOM.** *Ordinary Kriging (OK)*. OK is based on the  
 164 spatial autocorrelation and second-order stationary hypothesis [32], using the  
 165 semivariance function for calculation and analysis according to the principle of  
 166 minimum error to realize the optimal unbiased linear estimation of the unknown  
 167 region by using the data of known sampling points in a limited region. The  
 168 semivariance function formula is defined as follows.

$$\gamma(h) = \frac{1}{2N(h)} \sum_{i=1}^{N(h)} [Z(x_i) - Z(x_i + h)]^2 \quad (1)$$

169 where  $\gamma(h)$  is the semivariogram value,  $h$  is the lag between the two  
 170 locations,  $N(h)$  is the total number of point pairs when the interval is equal to  $h$ ,  
 171 and  $Z(x_i)$  and  $Z(x_i + h)$  are the measured values of the regional variables at  
 172  $x_i$  and  $x_i + h$ , respectively.

173 *Multiple Linear Regression (MLR) & Regression Kriging (RK)* RK combines  
174 MLR and OK interpolation [33]. The RK result consists of two parts: the trend  
175 item and the residual item. The trend item was obtained using the MLR model.  
176 The regression method used in this study is the input method. The MLR  
177 formula was expressed as follows:

$$y_i = \beta_0 + \sum_{i=1}^m \beta_i x_i + \varepsilon_i \quad (2)$$

178 where  $y_i$  is the predicted value of the model,  $\beta_0$  is the intercept,  $\beta_i$  is the  
179 regression coefficient,  $x_i$  is the independent variable, and  $\varepsilon_i$  is the model  
180 residual.

181 The residual generated by the prediction of the multiple linear regression  
182 model is estimated using the OK method, and the residual item is obtained.  
183 The trend and residual items were added to obtain the prediction result of the  
184 RK model. The RK formula was calculated as follows:

$$Z = m(x_i) + e(x_i) \quad (3)$$

185 where  $Z$  is the predicted value of the RK model,  $m(x_i)$  is the predicted item  
186 obtained by the MLR model, and  $e(x_i)$  is the residual item composed of the  
187 MLR model residual estimated by OK.

188 *Geographically Weighted Regression (GWR) & Geographically Weighted*  
189 *Regression Kriging (GWRK)*. GWRK is a combination of the GWR model and  
190 the OK method, which is similar to RK [34], and the trend item in the RK  
191 method is obtained by a regression item. The trend item in the GWRK method  
192 was simulated by the GWR model. The RK model is a global regression model,

193 while GWRK is a local regression model that is considered an improvement of  
194 the former. The relationship between variables is not considered in the  
195 modeling of MLR models, which are affected by spatial location, whereas  
196 GWR deals with the problem of spatial non-stationary characteristics by  
197 introducing the spatial location of sampling points and establishing local  
198 regression equations in the spatial range [35]. The regression coefficients of  
199 the GWR model change according to different spatial locations.

200 If there are  $n$  observation points in total, the position of each observation point  
201 is  $(u_i, v_i)$ , and there are  $m$  variables involved in the modeling, then the GWR  
202 model is expressed as follows:

$$y_i = \sum_{i=0}^n \sum_{j=0}^m \beta_j(u_i, v_i) x_{ij} + \varepsilon_i \quad (4)$$

203 where  $x_{ij}$  is the  $j$  th variable of observation point  $i$ ,  $\beta_j(u_i, v_i)$  is the  
204 regression coefficient of the  $j$  th independent variable at the position of  $(u_i, v_i)$ ,  
205  $\varepsilon_i$  is the random error term, and  $y_i$  is the dependent variable.

206 In GWR analysis, the Gaussian kernel and bisquare kernel functions are  
207 generally used to determine the spatial weight [36]. In our model analysis,  
208 different types of kernel functions were used according to the distribution of  
209 different observation points. When the distribution of the observation points is  
210 uniform, a fixed kernel function is used. When the distribution of observation  
211 points was uneven, the effect of the adaptive kernel function was better. Owing  
212 to the uneven distribution of sampling points in this study, an adaptive  
213 Gaussian kernel function was used for modeling. In addition, there is another

214 important indicator in the GWR model: effective bandwidth. An optimal  
215 bandwidth is vital for the accurate description of spatial features. The effective  
216 bandwidth is a smooth parameter: if the effective bandwidth is too wide, the  
217 parameters of the entire study area may become too similar and cover up the  
218 local details of the variables; if the effective bandwidth is too narrow, it will  
219 cause too many local spatial variations, and it is difficult to identify the spatial  
220 laws between variables. The determination methods of effective bandwidth  
221 include Akaike information criterion (AIC), corrected Akaike information  
222 criterion (AICc), Bayesian information criterion (BIC), and others. GWR  
223 analysis is sensitive to the bandwidth selection of specific weight function.  
224 Therefore, this study used the AICc to determine the model bandwidth. The  
225 model simulation is based on the AICc minimization principle.

226

227 *Multi-scale Geographically Weighted Regression (MGWR) & Multi-scale*  
228 *Geographically Weighted Regression Kriging (MGWRK)*. MGWRK is a  
229 combination of MGWR models and the OK interpolation method. MGWRK is  
230 an improvement of the GWRK method, in which all independent variables use  
231 the same effective bandwidth and the same spatial weight matrix. In the  
232 MGWR model, each independent variable has a different bandwidth. It  
233 considers the different spatial scales of spatial non-stationary characteristics  
234 between different independent variables, that is, multiple scales. The MGWR  
235 model is described as follows [27]:

$$y_i = \sum_{i=0}^n \sum_{j=0}^m \beta_{bwj}(u_i, v_i)x_{ij} + \varepsilon_i \quad (5)$$

236 where  $\beta_{bwj}$  is the regression coefficient corrected by the effective bandwidth of  
 237 the  $j$  th independent variable.

238 **Model Evaluation.** The mean error (ME), mean absolute error (MAE), root  
 239 mean square error (RMSE), and model prediction accuracy (ACC) were used  
 240 to evaluate the model accuracy [37, 38], which were calculated as follows:

$$ME = \frac{1}{n} \sum_{i=1}^n [Z(x_i) - \hat{Z}(x_i)] \quad (6)$$

$$MAE = \frac{1}{n} \sum_{i=1}^n [|Z(x_i) - \hat{Z}(x_i)|] \quad (7)$$

$$RMSE = \sqrt{\frac{1}{n} \sum_{i=1}^n [Z(x_i) - \hat{Z}(x_i)]^2} \quad (8)$$

$$ACC = \left[ 1 - \frac{1}{n} \sum_{i=1}^n \left| \frac{\hat{Z}(x_i) - Z(x_i)}{Z(x_i)} \right| \right] \quad (9)$$

241 where  $n$  is the number of observation points used for verification,  $Z(x_i)$  is the  
 242 measured value, and  $\hat{Z}(x_i)$  is the predicted value of the model. ME, MAE, and  
 243 RMSE values nearer to zero and higher ACC values indicate a better  
 244 prediction effect.

245

## 246 Results

247 **Selection of Environmental Covariates.** Many environmental factors affect  
 248 SOM. In this study, ten indicators, including slope, aspect, TRI, PC, TWI,  
 249 elevation, TEM, PRE, NPP, and NDVI were selected to study the impact of

250 each index on SOM. The spatial distribution of environmental covariates is  
251 shown in Figure 2, and the descriptive statistics of the environmental  
252 covariates are shown in Table 2.

253 The coefficient of variation (CV) is the ratio of the standard deviation to the  
254 mean, which can be used to reflect the spatial variation level of each index.  
255 When  $CV < 10\%$ , there is a weak variation; when  $10\% < CV < 100\%$ , it shows  
256 moderate variation; and when  $CV > 100\%$ , there is a strong variation [39].  
257 Table 2 shows that the coefficient of variation in some indicators belongs to  
258 weak variability, including elevation, TEM, PRE, and NDVI; among the  
259 indicators that belong to moderate variability, there are slope, aspect, TRI, and  
260 TWI; likewise, NPP, SOM, and PC are strongly variable.

261 In the process of modeling, selecting multiple variables may lead to the  
262 problem of multicollinearity between variables; that is, there is a high  
263 correlation between different variables, resulting in information redundancy,  
264 reducing model accuracy, and increasing calculation time. Therefore, the  
265 necessary condition for modeling each regression model is that there is no  
266 multicollinearity between the independent variables. Generally, the variance  
267 inflation factor (VIF) and tolerance are used to diagnose whether the data are  
268 multicollinear. Tolerance is the reciprocal of the variance inflation factor. When  
269  $VIF \geq 10$  and  $\text{tolerance} \leq 0.1$ , there is a serious collinearity problem between  
270 the variables. In this study, VIF and tolerance were used to diagnose the  
271 collinearity problem of these models, and the results are shown in Table 3. The

272 VIF of each variable was less than 10, and the tolerance was greater than 0.1,  
273 therefore, there were no serious collinearity problems in the model.

274 The final fitting model of MLR is:

$$\begin{aligned} 275 \quad \text{SOM} &= 16.654 + 0.023 * \text{Slope} + 0.002 * \text{Aspect} - 0.025 * \text{TRI} + 1.667 * \text{PC} + 0.049 * \text{T} \\ 276 \quad \text{WI} &- 0.007 * \text{Elevation} - 0.571 * \text{TEM} - 0.001 * \text{PRE} + 0.005 * \text{NPP} + 2.180 * \text{NDVI} \\ 277 \quad &(10) \end{aligned}$$

278 where SOM is soil organic matter, TRI is topographic relief index, PC is  
279 plane curvature, TWI is topographic wetness index, TEM is annual mean  
280 temperature, PRE is annual mean precipitation, NPP is the annual NPP, and  
281 NDVI is the annual NDVI. The variance analysis of the MLR model shows that  $f$   
282  $= 2.936$ ,  $P = 0.001$ , the model is statistically significant [39], and the regression  
283 equation is effective. GWR and MGWR also use the same variables to build  
284 the model.

285

#### 286 **Comparison of MLR, GWR, and MGWR Models in Terms of Accuracy.**

287 Table 4 compares the effects of the MLR, GWR, and MGWR models. RSS,  
288 AICc, and R2 are typically used to evaluate the performance of the model. The  
289 smaller the RSS and AICc, and the larger the R2 value, the higher the model  
290 accuracy. Combining various accuracy indicators, we concluded that the  
291 MGWR model was the most accurate, the GWR model was the second most  
292 accurate, and the MLR model was the least accurate.

293 **OK, RK, GWRK, and MGWRK Modeling.** The residuals of each model and

294 SOM were fitted with a spatial semivariogram, and the model parameters and  
295 optimal models are shown in Table 5. The best-fitting model for MGWR  
296 residuals is the spherical model, whereas the fitting models of other types are  
297 exponential models. The nugget value reflects the spatial heterogeneity  
298 caused by random errors in the sampling scale. The sill value represents the  
299 total variation intensity of the variables in the study area. A greater sill value  
300 indicates higher total heterogeneity in the system. The model range reflects  
301 the maximum distance of the spatial autocorrelation. The range of each model  
302 is between 240 and 640 m, the range of the MLR model residual is the  
303 smallest, and the range of the residual MGWR model is the largest. Nugget/sill  
304 is the ratio of the nugget value to the sill value, which is close to 1, indicating  
305 that the variation in these variables within the study area is constant. Generally,  
306 a nugget/sill value  $> 75\%$  indicates that the spatial variation is mainly affected  
307 by random factors. A value between  $25\%$  and  $75\%$  indicates that the variable  
308 has a moderate spatial autocorrelation. The variable is affected by the regional  
309 structure factors and random factors. A value of  $< 25\%$  indicates that the  
310 variables have strong spatial autocorrelation, mainly structural variation [32].  
311 The nugget/sill of the OK, MLR, GWR, and MGWR residuals were  $14.87\%$ ,  
312  $13.56\%$ ,  $13.98\%$ , and  $7.72\%$ , respectively, all of which were less than  $25\%$ ,  
313 indicating strong spatial autocorrelations. The residuals of each model were  
314 interpolated using their own semivariogram to obtain the spatial distribution  
315 map of the residuals (Figure 3).

316 The spatial distribution of MLR residuals was different from that of the  
317 other two models. The MLR residuals are generally low in the west, southwest,  
318 and southeast, and the high and low values clearly cluster. The spatial  
319 distribution of the GWR model residuals is a staggered distribution of high and  
320 low values. The staggered distribution of the MGWR model residuals is more  
321 obvious than that of the GWR model, and the phenomenon of “fragmentation”  
322 is more serious than that of the GWR model. The aggregation degree of the  
323 high and low values of residual spatial distribution in the MGWR model is  
324 weaker than that in the MLR and GWR models. From the residual distribution  
325 characteristics of these three models (Figure 3), the residual range is also  
326 different. The MLR residual range was the largest, while the MGWR residual  
327 range was the smallest. That is, the overall error caused by the MLR model  
328 was the largest, and the overall error caused by the MGWR model was the  
329 smallest. Most of the residual value ranges of the MGWR model are stably  
330 distributed between -2.23 and 1.25. From the perspective of residuals, the  
331 MGWR model performed the best, followed by GWR and MLR, respectively.

332

### 333 **Spatial Prediction of Soil Organic Matter Based on Different Methods**

334 Based on the spatial prediction of organic matter by different methods (Figure  
335 4), the spatial distribution trends of SOM predicted by different methods are  
336 basically the same. The spatial pattern of SOM in the study area was low in the  
337 southwest and southeast and high in the middle and east. The prediction of

338 SOM using the MLR model has the smallest value range. It is difficult to reflect  
339 the spatial distribution detail of SOM, and the MLR model has the most  
340 information distortion, followed by the GWR model. the “fragmentation”  
341 phenomenon of OK model and MLR model are also obvious. The mapping  
342 effects of the RK, GWRK, MGWR, and MGWRK models are smoother than  
343 those of the OK and MLR models, and the MGWR model performs well in a  
344 single model. Prediction and mapping effects of GWRK and MGWRK are more  
345 refined, which provides more details than other models.

346

347 **Model Accuracy Evaluation** The accuracy of the seven prediction models  
348 was evaluated by calculating five indices: mean error (ME), mean absolute  
349 error (MAE), root mean square error (RMSE),  $R^2$ , and evaluation accuracy  
350 (ACC). ME is an index to measure the deviation degree of model predictions,  
351 the closer it is to 0, the better the prediction effect. According to ME, the  
352 models ranked accordingly from best prediction effect to worst: MGWRK>  
353 GWRK>RK > OK > GWR > MLR. MAE and RMSE are indicators for  
354 measuring the prediction accuracy of the model. RMSE is sensitive to  
355 particularly large or small errors in the prediction results. The smaller the MAE  
356 and RMSE values, the better the prediction effect of the model was. The MAE  
357 values from small to large are GWRK> OK > RK > MGWRK > MGWR> GWR >  
358 MLR; and the RMSE values from small to large are GWRK> RK> OK >  
359 MGWRK> MGWR> GWR > MLR.  $R^2$  indicates the degree of coincidence

360 between the predicted value and the real value of the model. The order of  $R^2$   
361 values from large to small are GWRK > OK > RK > MGWRK > MGWR > GWR >  
362 MLR. In addition to the above four indicators, ACC is also introduced to  
363 evaluate model accuracy. ACC values closer to 1 indicate better model  
364 accuracies. According to the ACC index, the accuracy of the models rank  
365 accordingly from best to worst: GWRK > RK > OK > MGWRK > MGWR > GWR >  
366 MLR. Except for the unstable performance of individual models in the  
367 evaluation indicators, the performance trends of the models are generally the  
368 same, with the best performance of GWRK and the worst performance of MLR.

369

### 370 **Spatial Distribution of Regression Coefficients of Soil Organic Matter**

371 **Influencing Factors Based on MGWR Model.** According to the MLR

372 equation of SOM, SOM is positively correlated with slope, aspect, PC, TWI,

373 NPP, and NDVI, and negatively correlated with TRI, elevation, TEM, and PRE,

374 and there was only one regression coefficient on the global scale. In fact, the

375 influential extent of influencing factors on SOM cannot be constant in space,

376 and the relationship between dependent variables and independent variables

377 will change with geographical location, that is, with spatial non-stationarity [40].

378 The MGWR model performed better than the GWR model. Therefore, the

379 MGWR model was used to study the spatial distribution of the standardized

380 regression coefficients of different influencing factors. As shown in Figure 5,

381 the regression coefficients and positive or negative correlations between

382 different influencing factors and SOM are different at different spatial locations.  
383 The MGWR model considers the nonlinear relationship between SOM and  
384 influencing factors.

385

## 386 **Discussion**

387 When exploring the accuracy of each regression model, the MLR model,  
388 as a global model, only considers the numerical relationship between variables  
389 and does not consider that the relationship between variables will also change  
390 owing to the change in spatial location. In the MLR model, although the  
391 regression equation obtained is statistically significant, the regression equation  
392 obtained does not have an effective guiding significance. MLR models have a  
393 low model fitting degree and ignore the spatial non-stationary characteristics  
394 between SOM and its environmental auxiliary variables at the sampling sites;  
395 therefore, its accuracy proved the worst, compared to the other models  
396 examined. As local models, GWR and MGWR models can be regarded as an  
397 improvement of the MLR model. They consider the non-stationary  
398 characteristics between variables. The AICc values of the MLR, GWR, and  
399 MGWR models are 15 016.906, 14 973.07, and 14 872.466, respectively.  $R^2$   
400 increased slightly from 0.101 (GWR) to 0.162 (MGWR). Although the fitting  
401 degree is still low, in large-scale research areas, the accuracy is greatly  
402 improved when compared with the MLR global model (0.013). The MGWR  
403 model has a higher precision than the GWR model owing to its use of multiple

404 scales; the variables in the MGWR model have different bandwidths, but each  
405 variable of the GWR model shares one bandwidth. The MGWR model can  
406 better explain the relationship between the independent and dependent  
407 variables than the GWR model.

408 In the residual distribution range among models, that of the MGWR model  
409 is the smallest overall, and the interleaving of high and low values is not as  
410 serious as that of the MLR and GWR models, indicating that the multi-scale  
411 function of the MGWR model plays an obvious role in reducing the spatial  
412 residual. Because the effective bandwidth between various variables in the  
413 GWR model is the same, the phenomenon of fragmentation is more serious  
414 than in the MGWR model. As the global model, MLR has the largest residual  
415 range, which shows that the local regression model can better reduce the  
416 residual item of the regression model than the global model.

417 In terms of the visualization effect of the spatial prediction of SOM, the  
418 mapping of the RK model is smoother than that of the other hybrid models. The  
419 reason may be that the MLR model only retains the spatial trend of large-scale  
420 SOM in the prediction process, and its prediction effect is poor in narrow space  
421 and small scale. The MLR model cannot reflect variations in local details and  
422 excludes too many local features, and the mapping of the MLR model has high  
423 information distortion. Comparing the GWR and MGWR models, the latter has  
424 a better mapping effect. These two models are superior to the MLR model  
425 because they consider the spatial non-stationary characteristics of SOM. The

426 MGWR, GWRK, and MGWRK models are based on the improvement of the  
427 local regression model, and the model details perform well. The MGWR and  
428 MGWRK models also consider the scale problem based on local theory.  
429 MGWRK is the next step, and it shows more details in the spatial prediction  
430 distribution of the model than the other six models.

431 Seven models were evaluated and discussed. Comparing the index  
432 evaluation accuracy, ACC, of each model, the GWRK method is the best. As a  
433 common spatial prediction method, OK also achieves good accuracy, which is  
434 flush with the RK model. Although the MGWR model is superior to the GWR  
435 model, its accuracy is inferior to that of the GWRK model. Combined with the  
436 analysis of the residual distribution map, although the local regression model  
437 better reduces the residual term of the regression model, multi-scale is both an  
438 advantage and an interference in spatial prediction. The prediction accuracy of  
439 MGWRK reached 47.72% for the OK method, 47.72% for the RK method, and  
440 40.08% for the GWRK method. Many studies show that the GWRK model  
441 achieves better prediction accuracy in most cases because the GWR model is  
442 more mature [38, 41]. As a new improved model, although the accuracy of  
443 MGWR model needs to be improved, it still provides a new idea for spatial  
444 prediction and has a great exploration value.

445 In terms of the spatial distribution of regression coefficients, the regression  
446 coefficients of most environmental variables have the same correlation in the  
447 overall environment of the study area; only the strength of the regression

448 coefficients is different in space. It is inferred that TRI, TEM, and PRE may  
449 have a strong effect on the change in SOM according to the size of the  
450 regression coefficients. The regression coefficients of TRI, TWI, and NPP are  
451 mixed with positive and negative values. The spatial positive and negative  
452 correlations between SOM and these three indicators were different. The  
453 regularity of this situation is not obvious, which may be related to the complex  
454 landforms and vegetation distribution in Lingshi County. Slope, aspect, and  
455 plane curvature are positively correlated with SOM, which may restrict human  
456 activities and reduce the interference of human factors and SOM [42].  
457 Elevation and PRE are negatively correlated with SOM, which may be  
458 because the lower the altitude, convenient transportation, flat terrain, and the  
459 application of chemical fertilizer and organic fertilizer provided good conditions  
460 to the SOM, so the content of SOM is high [7, 43]; due to the influence of  
461 leaching, the rainfall is greater, and more SOM will be lost [44].

462         Although the new MGWRK method improves the prediction accuracy of  
463 the model in part, this improvement is not obvious and fails to achieve the  
464 expected effect. The operation cost of the MGWRK model may be higher than  
465 that of OK; when the study area is large and the sampling point density is high,  
466 the OK method can also fully provide good support for spatial prediction, and  
467 the process of mapping is simpler and quicker, but in front of the manpower  
468 and material resources saved by accurately predicting SOM, the operation  
469 cost of the model can be ignored. Composite models may have higher

470 accuracy than unitary models in theory; they are not as mature as common  
471 models and do not have as widespread usage. However, the MGWR model  
472 has the advantage of revealing spatial non-stationary characteristics that other  
473 models do not. Although the application effect of MGWRK model in soil spatial  
474 prediction is unsatisfactory, it can still be used as a new progress in the  
475 application of regression method in spatial prediction, but it needs to explore  
476 more suitable application scenarios.

477       The prediction accuracy of the regression model was highly sensitive to  
478 the correct selection of auxiliary variables. There are many factors influencing  
479 SOM through a complex mechanism. It is crucial to scientifically and  
480 reasonably select the influencing factors of SOM to improve the accuracy of  
481 the model.

482       The study only selected some environmental variables as auxiliary  
483 variables for modeling and did not consider human factors. The spatial  
484 variation in SOM is also affected by human activities and other factors. In a  
485 follow-up study, the cultivation management measures should be quantified  
486 and included in the scope of model measurements to further improve the  
487 influence mechanism of SOM, to improve the accuracy of simulation and  
488 prediction.

489       After the standardization of the MGWR model, this study only makes a  
490 visual study on the regression coefficient, and it does not involve an in-depth  
491 examination of the local  $R^2$  and other indicators. Subsequent studies can

492 deeply excavate other indicators of the standardized MGWR model.

493

## 494 **Conclusion**

495 In summary, this study compared the performance of seven different methods  
496 (OK, MLR, RK, GWR, GWRK, MGWR, and MGWRK) in the spatial prediction  
497 of SOM in Lingshi County, Jinzhong City, Shanxi Province, and applied the  
498 MGWR model to explore the factors influencing cultivated SOM.

499 In terms of the spatial prediction of SOM, the general trend of these models is  
500 the same, only differing in the granular degree of the mapping effect. The  
501 overall spatial pattern of SOM in the study area was low in the southwest and  
502 southeast, and high in the middle and east. The prediction accuracy of the  
503 GWRK model was the highest, and that of the MLR model was the worst. The  
504 accuracy of the RK model was greatly improved after the residual of the MLR  
505 model was estimated using the OK method. In general, the hybrid models (RK,  
506 GWRK, and MGWRK) were better than the single models (MLR, GWR, and  
507 MGWR).

508 The MGWR model achieves a different spatial distribution of regression  
509 coefficients, breaks the limitation of global correlation coefficients, uses  
510 different optimal bandwidths for each variable, which is more in line with the  
511 actual situation, and more accurately describes the spatial nonstationary  
512 characteristics of each variable. It also shows a complex nonlinear relationship  
513 between SOM and the influencing factors.

514

515

516

517

518

519

520

521

522

523

524

525

526

527

528

529

530

531

532

533

534

535

536 **References**

- 537 1. Sun, Y., Wang ,W., Li, G. Spatial distribution of forest carbon storage in Maoershan  
538 region, Northeast China based on geographically weighted regression kriging model.  
539 *Chin. J. Appl. Ecol.* **30**, 1642-1650 (2019).
- 540 2. Wang, S., Zhou, C., Li, K., Zhu, S., Huang, F. Analysis on Spatial Distribution  
541 Characteristics of Soil Organic Carbon Reservoir in China. *Acta Geogr. Sin.* 533-544  
542 (in Chinese) (2000).
- 543 3. Simbahan, G.C., Dobermann, A., Goovaerts, P., Ping, J., Haddix, M.L.  
544 Fine-resolution mapping of soil organic carbon based on multivariate secondary data.  
545 *Geoderma* **132**, 471-489 (2006).
- 546 4. Wu, T., Schoenau, J.J., Li, F., Qian, P., Zhang, S., Malhi, S.S., Wang, F. Concepts and  
547 relative analytical techniques of soil organic matter. *Chin. J. Appl. Ecol.* 717-722 (in  
548 Chinese) (2004).
- 549 5. Zamulina, I.V., Gorovtsov, A.V., Minkina, T.M., Mandzhieva, S.S., Bauer, T.V. Soil  
550 organic matter and biological activity under long-term contamination with copper.  
551 *Environ. Geochem. Health.* (2021).
- 552 6. Zhang, J.; Sayer, E.J.; Zhou, J.; Li, Y.W.; Li, Y.X.; Li, Z.; Wang, F. Long-term  
553 fertilization modifies the mineralization of soil organic matter in response to added  
554 substrate. *Sci. Total Environ.* 798 (2021).
- 555 7. Yang, J.; Han, X.; Huang, J.; Pan, Q. The dynamics of soil organic matter in cropland  
556 responding to agricultural practices. *Acta Ecol. Sin.* 787-796 (in Chinese) (2003).
- 557 8. Hanli, Q.; Xiubo, S.; Huazhou, C.; Jingyi, L.; Shaoyong, H. Effective prediction of soil

- 558 organic matter by deep SVD concatenation using FT-NIR spectroscopy. *Soil Tillage*  
559 *Res.* **215**,(2022): doi:10.1016/J.STILL.2021.105223.
- 560 9. Zhao, M., Liu, B., LV, H., Li, D., Zhang, G. Spatial modeling of soil organic matter over  
561 low relief areas based on geographically weighted regression. *Trans. Chin.*  
562 *Soc. Agric. Eng.* **35**, 102-110 (in Chinese) (2019).
- 563 10. Eldeiry, A.A., Garcia, L.A. Comparison of Ordinary Kriging, Regression Kriging, and  
564 Cokriging Techniques to Estimate Soil Salinity Using LANDSAT Images. *ASCE J.*  
565 *Irrig. Drain. Div.* **136**, 355-364 (2010).
- 566 11. Mcbratney, A.; Santos, M.; Ma, B.J.G. On Digital Soil Mapping. *Geoderma.* **117**, 3-52  
567 (2003).
- 568 12. Chen, F., Qin, F., Li, X., Peng, G. Inversion for spatial distribution of soil organic  
569 matter content based on multivariate geostatistics. *Trans. Chin. Soc. Agric. Eng.* **28**,  
570 188-194+297 (2012).
- 571 13. Li, Q., et.al. Spatially distributed modeling of soil organic matter across China: An  
572 application of artificial neural network approach. *Catena.* **104**, 210-218 (2013).  
573 doi:10.1016/j.catena.2012.11.012.
- 574 14. Li, Q., et.al. Prediction of distribution of soil organic matter based on qualitative and  
575 quantitative auxiliary variables: a case study in Santai County in Sichuan Province.  
576 *Prog.Geogr.* **33**, 259-269 (2014).
- 577 15. Lian, G., Guo, X., Fu, B., Hu, C. spatial variability and prediction of soil nutrients on a  
578 county scale on the loess plateau—a case study of heng shan county,Shaanxi  
579 province. *Acta Pedol. Sin.* 577-584 (in Chinese) (2008).

- 580 16. Qi, Y., Wang, Y., Chen, Y., Liu, J., Zhang, L. Soil organic matter prediction based on  
581 remote sensing data and random forest model in Shaanxi province. *J. Nat. Resour.*  
582 **32**, 1074-1086 (in Chinese) (2017).
- 583 17. Zhang, S., et.al. Prediction of spatial distribution of soil nutrients using terrain  
584 attributes and remote sensing data. *Trans. Chin. Soc. Agric. Eng.* **26**, 188-194 (In  
585 Chinese) (2010).
- 586 18. López-Granados, F., Jurado-Expósito, M., Using geostatistical and remote sensing  
587 approaches for mapping soil properties. *Eur. J. Agron.* **23**, 279-289 (2005).
- 588 19. Duan, L., Guo, L, Zhang, H., Ju, Q. Prediction of spatial distribution of soil organic  
589 matter based on improved OK models: A case study of Honghuatao Town in Yidu  
590 City. *Chin. J. Eco-Agric.* **27**, 131-141 (in Chinese) (2019).
- 591 20. Hengl, T., Heuvelink, G., Stein, A. A generic framework for spatial prediction of soil  
592 variables based on regression-kriging. *Geoderma.* **120**, 75-93 (2004).
- 593 21. Niu, L., et.al. Research on China's surface urban heat island drivers and its spatial  
594 heterogeneity. *China Environ. Sci.* **2021**, 1-11.
- 595 22. Yu, f., Liu, J., Xia, L., Xu, Z., Long, X. Spatial Prediction Method of Farmland Soil  
596 Organic Matter in Weibei Dryland of Shaanxi Province. *Chin. J. Environ. Sci.* 1-13(in  
597 Chinese) (2021).
- 598 23. Ding, Y., et.al. Spatial distribution characteristics and influencing factors of soil  
599 organic carbon in Yihe River Basin based on GWR model *Acta Ecol. Sin.* **41**,  
600 4876-4885 (in Chinese) (2021).
- 601 24. Yang, S.-H., et.al. Mapping topsoil electrical conductivity by a mixed geographically

- 602 weighted regression kriging: A case study in the Heihe River Basin, northwest China.  
603 *Ecol. Indic.* **102**, 252-264(2019). doi:10.1016/j.ecolind.2019.02.038.
- 604 25. Liu, Y., Guo, L., Jiang, Q., Zhang, H., Chen, Y. Comparing geospatial techniques to  
605 predict SOC stocks. *Soil Tillage Res.* **148**,46-58(2015).doi:10.1016/j.still.2014.12.002.
- 606 26. Ye, H.; Huang, W.; Huang, S.; Huang, Y.; Zhang, S.; Dong, Y.; Chen, P. Effects of  
607 different sampling densities on geographically weighted regression kriging for  
608 predicting soil organic carbon. *Spatial Stat.* **20**, 76-91 (2017).  
609 doi:10.1016/j.spasta.2017.02.001.
- 610 27. Fotheringham, A.S., Yang, W., Kang, W. Multiscale Geographically Weighted  
611 Regression (MGWR). *Ann. Am. Assoc. Geogr.* **107**,1247-1265 (2017).  
612 doi:10.1080/24694452.2017.1352480.
- 613 28. Qiu, L.; Yang, C.; Lin, F; Yang, N.; Zheng, X.; Xu, H.; Wang, K. Spatial pattern of soil  
614 fertility in Bashan tea garden: A prediction based on environmental auxiliary variables.  
615 *Chin. J. Appl. Ecol.* **21**, 3099-3104 (in Chinese) (2010).
- 616 29. Jiang, Y.; Li, Q.; Zhang, X.; Liang,W. Kriging prediction of soil zinc in contaminated  
617 field by using an auxiliary variable. *Chin. J. Appl. Ecol.* 97-101 (in Chinese) (2006).
- 618 30. Zeng, C.; Yang, L.; Zhu, A.X.; Rossiter, D.G.; Liu, J.; Liu, J.; Qin, C.; Wang, D.  
619 Mapping soil organic matter concentration at different scales using a mixed  
620 geographically weighted regression method. *Geoderma.* **281**, 69-82 (2016).  
621 doi:10.1016/j.geoderma.2016.06.033.
- 622 31. Bao, S. Soil agrochemical analysis .3 rd ed.; China Agriculture Press: Beijing, China,  
623 25-38 (in Chinese) (2000).

- 624 32. Liu, A.; Wang,P.; Ding, Y. *Introduction to Geostatistics*; Science Press: Beijing,  
625 China, 82 (in Chinese) (2012).
- 626 33. Odeh, I.; Mcbratney, A.B.; Chittleborough, D.J. Further results on prediction of soil  
627 properties from terrain attributes: heterotopic cokriging and regression-kriging.  
628 *Geoderma* **67**, 215-226 (1995).
- 629 34. Yang, S.; Zhang, H.; Guo, L.; Ren, Y. Spatial interpolation of soil organic matter using  
630 regression Kriging and geographically weighted regression Kriging. Chinese. *Chin. J.*  
631 *Appl. Ecol.* **26**, 1649-1656 (in Chinese) (2015).
- 632 35. Griffith, D. Spatial-filtering-based contributions to a critique of geographically  
633 weighted regression (GWR). *Environment Planning A* **40**, 2751-2769 (2008).
- 634 36. Fotheringham; A.; S.; Charlton; M. Geographically weighted regression: a natural  
635 evolution of the expansion method for spatial data. *Environment Planning A.* **30**,  
636 1905-1927 (1998).
- 637 37. Yang, S., et.al. Predicting soil organic matter content in a plain-to-hill transition belt  
638 using geographically weighted regression with stratification. *Arch. Agron. Soil Sci.* **65**,  
639 1745-1757 (2019). doi:10.1080/03650340.2019.1576171.
- 640 38. Gao, L., et.al. Comparative Study on Spatial Digital Mapping Methods of Soil  
641 Nutrients Based on Different Geospatial Technologies. *Sustainability* **13**, (2021)  
642 doi:10.3390/su13063270.
- 643 39. Liu, H.; Mao, W.; Modern statistics. 2nd ed.; Sun Yat-sen University Press:  
644 Guangzhou, China (in Chinese) (2002).
- 645 40. Wang, X, et.al. comparing Interpolation Methods to Predict the Spatial Distribution of

- 646 Soil Available Phosphorus in the Mollisol Watershed of Northeast China. *Res. Soil*  
647 *Water Conserv.* **28**, 33-40 (2021).
- 648 41. Qiao, L., Zhang, W., Huang, M., Wang, G., Ren, J. Mapping of Soil Organic Matter  
649 and Its Driving Factors Study Based on MGWRK. *Chin. Agric. Sci.* **053**, 1830-1844  
650 (2020).
- 651 42. Liu, J., Xu, X., Simulating the effects of different management modes on the  
652 ecosystem services of agroecosystems: a case study of the Taihu Lake Basin, China.  
653 *Acta Ecol. Sin.* **39**, 9314-9324 (in Chinese) (2019).
- 654 43. Hu, Z., Liu, S., Shi, Z., Liu, X., He, F. Variations of Soil Nitrogen and Microbial  
655 Biomass Carbon and Nitrogen of *Quercus aquifolioides* Forest at Different Attitudes in  
656 Balangshan, Sichuan. *Forest Research* **25**, 261-268 (2012).
- 657 44. Pingshun, G., Mingzhu, H., Guangzu, B., Pengshan, Z., Qingxia, G. Spatial  
658 distribution characteristics of soil organic matter in Chinese herbal medicine planting  
659 area in Longxi County. *Agricultural Research in the Arid Areas.* **38**, 192-197+251 (in  
660 Chinese) (2020).

661

## 662 **Acknowledgements**

663 This study was funded by by State Key Laboratory of Integrative Sustainable  
664 Dryland Agriculture (in preparation) , Shanxi Agricultural University (No.  
665 202105D121008-1-6)

## 666 **Author Contributions**

667 Conceptualization, X.Z.; Methodology, X.Z., L.G. and L.Q.; Software, X.Z. and

668 L.G.; Validation, X.Z. and G.L.; Formal Analysis, G.W. and L.Y.; investigation,  
669 X.Z., L.G. and L.Q.; Resources, W.Z.; Data Curation, X.Z.; Writing—Original  
670 Draft Preparation, X.Z.; Writing—Review & Editing, W.Z. and X.Z.;  
671 Visualization, X.Z.; Supervision, W.Z.; Project Administration, W.Z. and M.H.;  
672 Funding Acquisition, W.Z. and M.H. All authors have read and agreed to the  
673 published version of the manuscript.

674 **Additional Information**

675 Competing Interests: The authors declare no competing interests.

676 **Data Availability Statement:** Publicly available datasets were analyzed in this  
677 study. These data can be found here: <https://www.resdc.cn> (accessed on 23  
678 April 2021); <http://www.gscloud.cn> (accessed on 23 April 2021).

679

680

681

682

683

684

685

686

687

688

689

690 **Table and Fig.**

Datatype	Index	Extraction methods
Terrain data	Aspect	Extracted from DEM through ArcGIS surface analysis function
	Slope	
	Topographic relief index, TRI	TRI=E max- E min
		E max Maximum elevation
		E min Minimum elevation
	Plan curvature, PC	Extracted from DEM through ArcGIS surface analysis function
	Topographic wetness index, TWI	Extracted from DEM through SAGA-GIS terrain analysis function
	Elevation	Extracted from DEM through ArcGIS spatial analysis tool
Meteorological	Annual mean precipitation, PRE	Interpolation software is ANUSPLIN (www.resdc.cn)
	Annual mean temperature, TEM	
Remote sensing data	The Annual Net primary productivity, NPP	Calculated based on GLO_PEM model。Unit: gC/m3 (www.resdc.cn)
	The Annual Normalized differential vegetation index, NDVI	Calculated based on MVC method Through SPOT/VEGETATION NDVI remote sensing data, NDVI is the maximum value of monthly NDVI in a year. (www.resdc.cn)

691 **Table 1. Environmental covariates and exaction method**

692

693

694

695

696

Index	Unit	Min	Max	Mean	S.D.	Variance	Coefficient of Variance(%)
Soil organic matter	g/kg	0.10	48.00	4.82	6.87	47.18	142.62
Slope	°	0.00	31.48	9.84	4.96	24.59	50.39
Aspect	°	-1.00	359.21	189.81	98.19	9641.52	51.73
Topographic relief index		7.00	150.00	54.97	20.11	404.47	36.59
Plan curvature		-0.71	1.10	0.01	0.17	0.03	1240.56
Topographic wetness index		4.86	22.04	7.29	2.40	5.76	32.95
Elevation	m	674.00	1385.00	978.71	93.69	8778.63	9.57
Annual mean temperature	°C	8.98	12.38	10.74	0.49	0.24	4.55
Annual mean precipitation	mm	483.29	576.15	529.13	17.57	308.77	3.32

The Annual NPP	gC/m <sup>2</sup>	71.20	505.40	223.90	63.81	4071.88	28.50
The Annual NDVI		0.46	0.73	0.64	0.04	0.00	6.17

697 **Table 2.** Descriptive statistics of soil organic matter and environmental  
698 covariates

699  
700  
701

Index	Tolerance	VIF
Slope	0.369	2.711
Aspect	0.934	1.071
Topographic relief index	0.432	2.312
Plan curvature	0.866	1.154
Topographic wetness index	0.543	1.841
Elevation	0.195	5.120
Annual mean temperature	0.136	7.370
Annual mean precipitation	0.291	3.433
The Annual NPP	0.834	1.199
The Annual NDVI	0.720	1.389

702 **Table 3.** Multicollinearity test of models.

703

Model	RSS	AIC	AICc	R2	Adjust R2
MLR	104493.078	15014.766	15016.906	0.013	0.009
GWR	95172.649	14968.948	14977.07	0.101	0.063
MGWR	88684.105	14859.383	14872.466	0.162	0.116

704 **Table 4.** Accuracy diagnosis of regression models.

705

Type	Fitting-Model	Nugget(C0)	Sill(C0+C)	Range(m)	Nugget/Sill(C0/C0+C)
OK	Exponential model	7.1	47.75	250	14.87
MLR Residual	Exponential model	6.4	47.2	240	13.56
GWR Residual	Exponential model	6.1	43.63	290	13.98
MGWR Residual	Spherical model	3.1	40.13	640	7.72

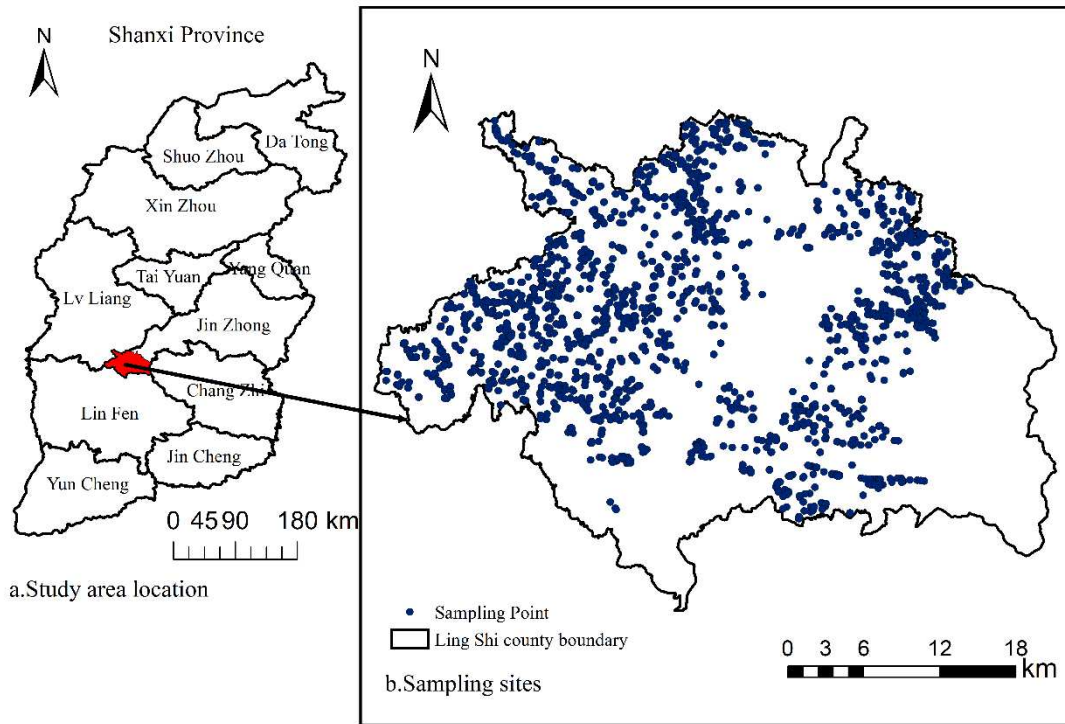
706 **Table 5.** Semivariance parameters of each model.

707

Model	ME	MAE	RMSE	R2	ACC
OK	0.0364	3.8997	5.5864	0.4065	-0.8298
MLR	-0.3714	5.3039	6.8970	0.0122	-1.6960
RK	0.0229	3.9039	5.5777	0.4064	-0.8275
GWR	0.0912	4.7905	6.5767	0.1058	-1.2373
GWRK	0.0127	3.7022	5.2862	0.4840	-0.7369
MGWR	-0.1003	4.5931	6.3483	0.1630	-1.2032

708

**Table 6.** Comparison of prediction accuracy of seven models.



709

**Figure 1.** The study area and the sampling point distribution

710

711

712

713

714

715

716

717

718

719

720

721

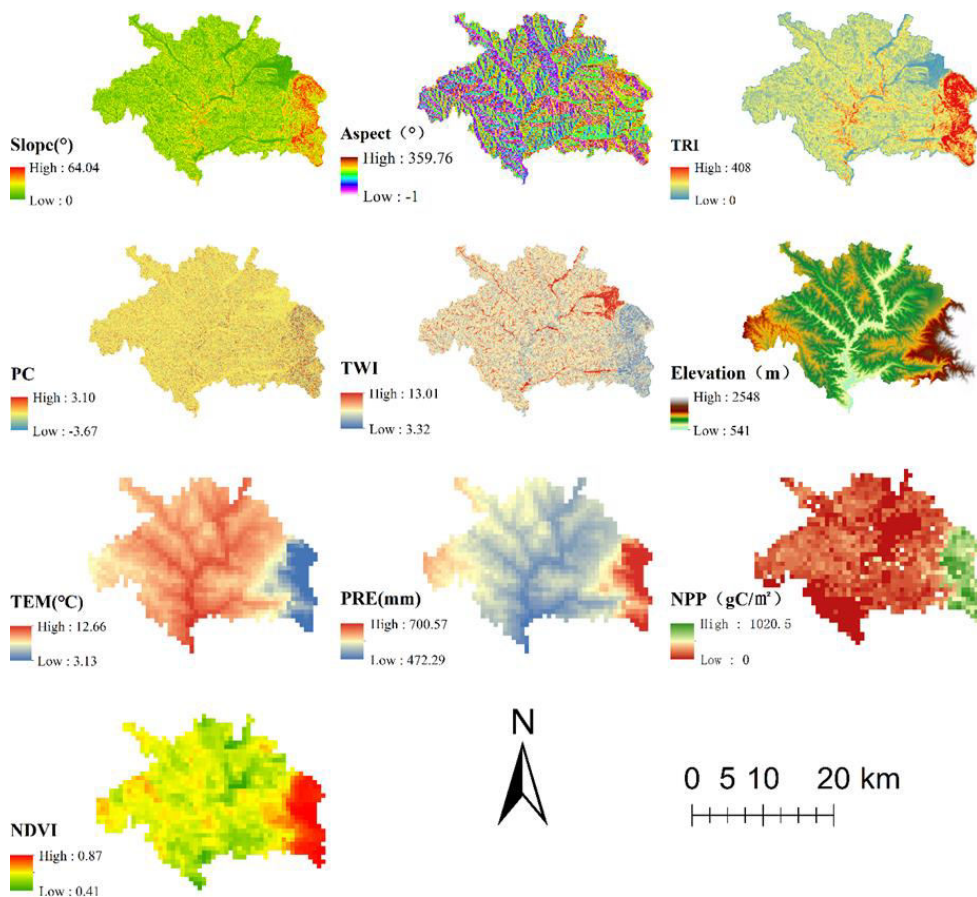
722

723

724

725

726



727

728

729 **Figure 2.** Spatial distribution of environmental covariates

730

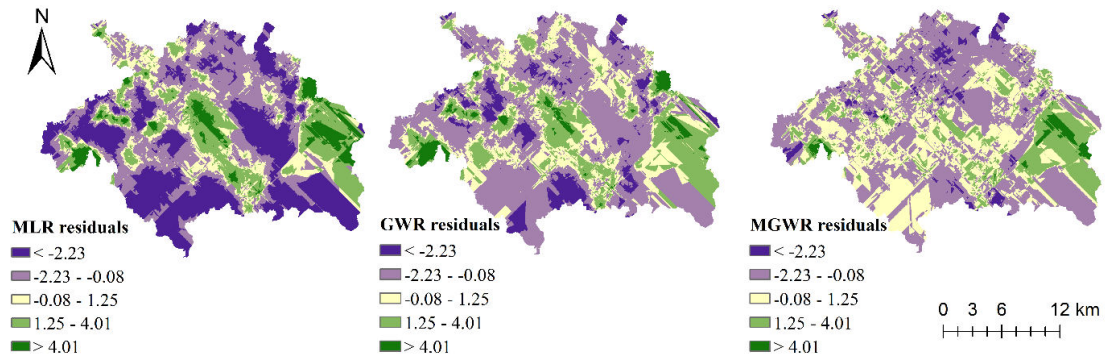
731

732

733

734

735



736

737

738

739

740 **Figure 3.** Spatial distribution map of MLR, GWR, and MGWR residuals

741

742

743

744

745

746

747

748

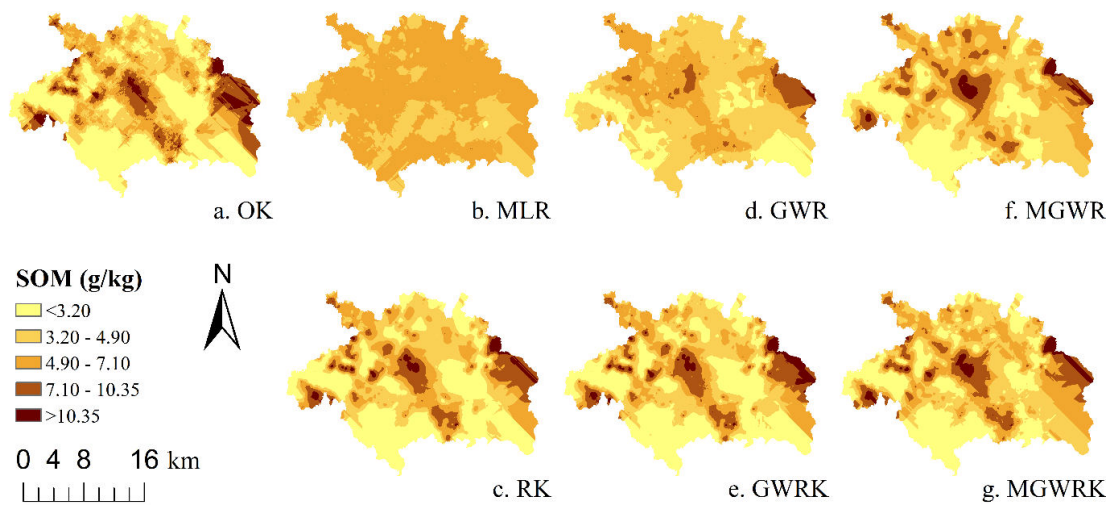
749

750

751

752

753



754 **Figure 4.** Prediction of spatial distribution of soil organic matter by different  
755 methods

756

757

758

759

760

761

762

763  
 764  
 765  
 766  
 767  
 768  
 769  
 770  
 771  
 772  
 773  
 774  
 775  
 776  
 777  
 778  
 779  
 780  
 781  
 782  
 783  
 784  
 785

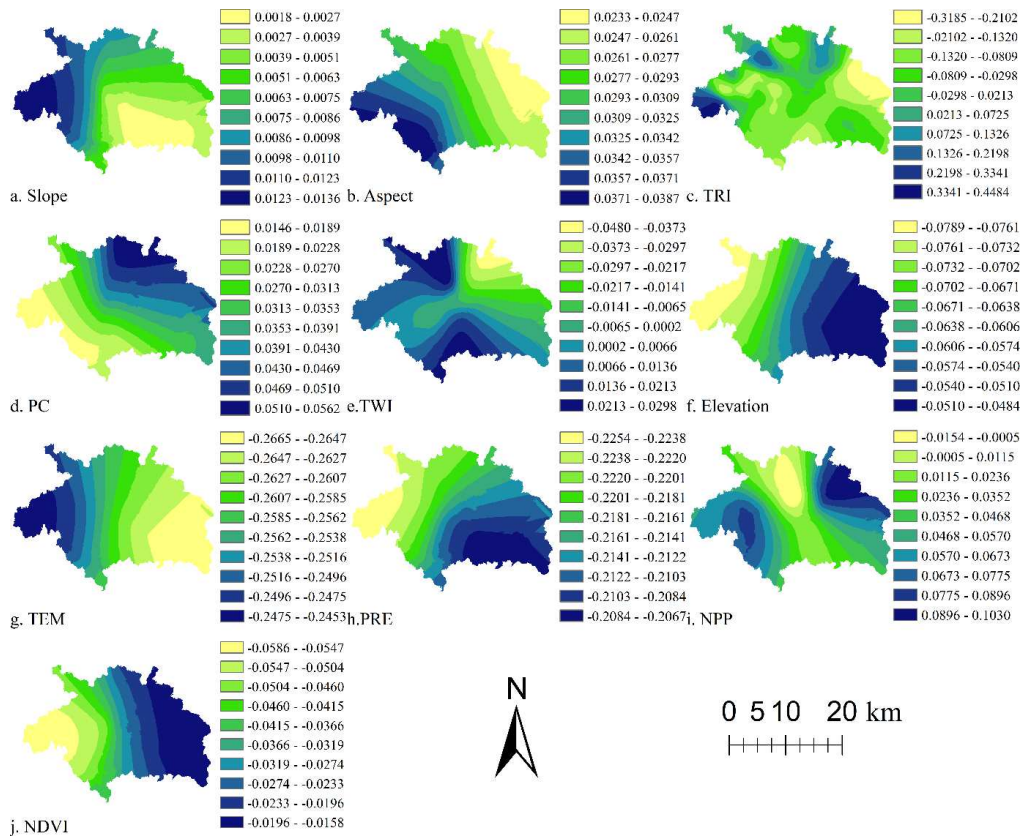


**Figure 5.** Spatial distribution of normalized regression coefficients of influencing factors based on MGWR